Supplement of

Predicting the climate impact of aviation for en-route emissions: The algorithmic climate change function submodel ACCF 1.0 of EMAC 2.53

Emma Klingaman and Keith Shine

University of Reading, Department of Meteorology, RG6 6AH Reading, United Kingdom

Contrail algorithmic Climate Change Function derivation

This document describes the dataset used to derive the contrail algorithmic climate change functions (aCCFs; Section S1) and the derivation of the aCCFs (Section S2).

S1. Calculation of contrail radiative forcing from Lagrangian trajectory data

The method for producing the contrail RF dataset used in the analysis and derivation of the contrail environmental change functions (ECF) is described. The method is illustrated in Figure S1. Lagrangian trajectories are used to determine the lifetime of a contrail, the temperature, and position along the lifetime of the contrail. This information is used to calculate the contrail optical depth and solar zenith angle, which are required to calculate the contrail radiative forcing from the Schumann et al. (2012) parametric model. These steps are described in the following sub-sections.

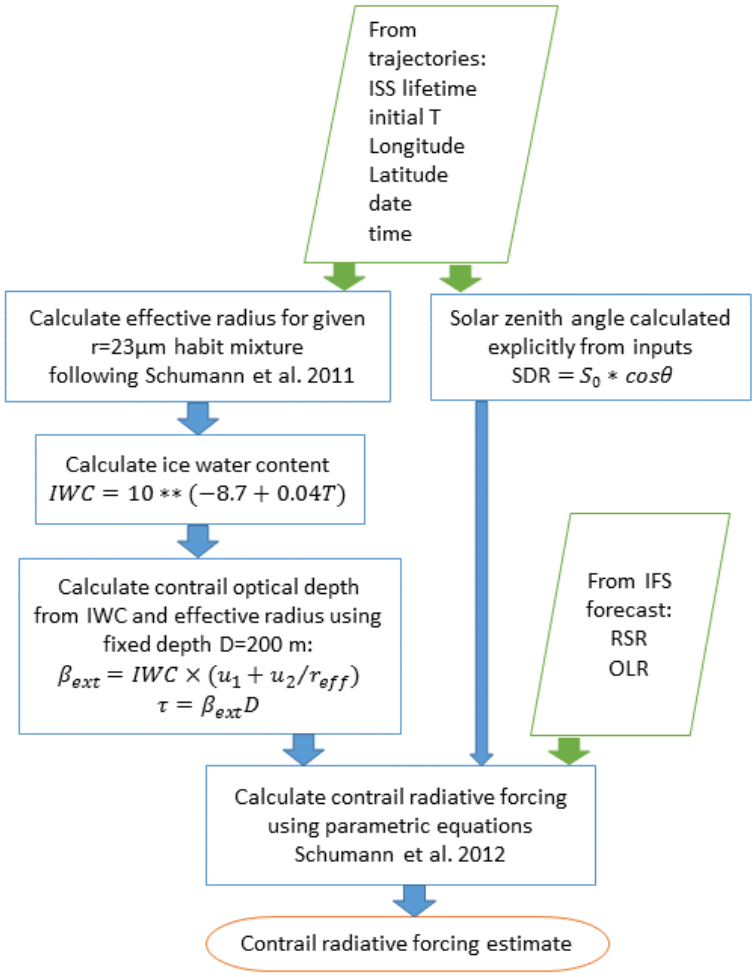

Figure S1: Flowchart illustrating the method used to calculate the contrail RF. Data input to the calculation are in green polygons and calculations are shown in blue rectangles.

Calculation of air parcel trajectories and contrail lifetime

Full details of the computation of the methodology used to calculated the trajectories are described in Irvine et al. (2014), and a summary is given here. Lagrangian trajectories (i.e., following the air parcel) were computed using ERA-Interim winds input to a trajectory model (Methven, 1997), which uses a fourth-order Runge-Kutta integration scheme. Trajectories were initialized from a grid covering the north Atlantic (35 °N – 60 °N, 0 °W – 70 °W) with 1 ° horizontal spacing and from three vertical levels: 300 hPa (FL300), 250 hPa (FL340) and 200 hPa (FL390). Trajectories were initialized 12-hourly every day during the winters (December, January and February) of 1994-95, 1995-96, and 2003-04; the winters were chosen to cover the range of synoptic weather conditions experienced over the north Atlantic in winter.

To identify trajectories where contrail formation would have been possible at the time the trajectory was initialised, two thresholds were applied: relative humidity with respect to ice above 98% and a temperature below

235 K. The contrail lifetime was estimated by analysing each of these trajectories to see how long these conditions persisted for. This estimate is likely to be an upper bound on contrail lifetime since processes such as sedimentation and dissipation are not accounted for. The trajectory data has a time resolution of 6 hours. Trajectories, where the conditions for contrail formation were satisfied at only the initial point, were given a lifetime of 3 hours, trajectories, where conditions were satisfied at the first two points, were given a lifetime of 6 hours, three points 12 hours, and so on. Various meteorological variables are available along the trajectories. The RF calculations in this study use temperature, location (latitude, longitude), date, and time.

Calculation of contrail properties

Contrail optical depth can be calculated at each point along the contrail trajectory from the ice water content, effective radius and contrail depth. Contrail ice water content, IWC, is calculated using an empirical Eq. (S1) from Schumann et al. (2017), which is derived from fits to observed contrail data.

$$IWC = 10 ** (-8.7 + 0.04T) \quad \text{(S1)}$$

This IWC calculation requires only the temperature *T* as input, which is taken from the trajectory data.

To estimate the contrail ice particle effective radius, we use data from observations of contrail effective radius as a function of contrail age presented in Figure 3 of Schumann et al. (2017). In-situ, remote sensing observations, as well as model simulations, show that an effective radius (r_{eff}) of around 10-50 microns is appropriate for contrail cirrus. The constituent ice particles would have different shapes (habits), which have different scattering properties. Table 2 of Schumann et al. (2011) lists a habit mixture of 30% solid hexagonal columns, 30% spatial bullet rosettes, and 40% droxtals for contrail cirrus ice particle radius of 23 microns. The conversion to effective radius for these particles is given in Table 1 of the same reference. The calculations below are performed separately for each of these ice particle habits.

Unterstrasser and Gierens (2010) present a simple formula for the extinction coefficient $ß_{ext}$ in terms of IWC and r_{eff}:

$$\beta_{ext} = IWC \times (u_1 + u_2/r_{eff}) \quad \text{(S2)}$$

where u_1=3.448m^2/kg and u_2=2.431x10^{-3}m^3/kg. The optical depth τ is then simply the product of the extinction coefficient and the contrail depth D:

$$\tau = \beta_{ext} D \quad \text{(S3)}$$

In REACT4C calculations, the initial contrail depth D was set to 200 m (Table 4 in Grewe et al. (2014a)). We assume a constant contrail depth with lifetime, which will result in an underestimate of the optical depth, particularly for longer-lived contrails. The extinction coefficient will vary along the trajectory as the temperature changes but note that the effective radius is constant.

Radiative forcing calculation

The RF calculation uses the parametric model developed by Schumann et al. (2012). The parametric model parameters are given as a function of ice particle habits, and the RF calculations are performed separately for each habit class, and the total RF is calculated as the sum of the contributions from the habit classes weighted by their contribution.

The longwave (LW) RF is dependent on the outgoing longwave radiation (OLR) at the top of atmosphere (TOA), contrail temperature, contrail optical depth and effective contrail ice particle radius. Note that additional complexity can be introduced into the model by accounting for the optical depth of cirrus cloud present above the contrail; for these calculations, we assume a cloud-free atmosphere above the contrail, so this parameter is set to zero. The OLR is not available as a parameter in the ERA-Interim data, so it is instead taken from short forecasts from the ECMWF IFS, where it is available as an accumulated value (rather than an instantaneous value) over the length of the forecast (6 or 12 hours). Using these parameters, the LW RF is calculated using Eq. (2) and (3) from Schumann et al. (2012). The model parameters for each habit type are given in Table 1 of Schumann et al. (2012).

The shortwave (SW) RF is dependent on the solar direct irradiance at TOA (SDR), solar zenith angle (SZA), contrail optical depth, reff and the effective albedo given by the ratio of the reflected solar radiation at TOA to the solar direct irradiance. As for the LW RF calculations, we assume a cloud-free atmosphere above the contrail, hence set the optical depth of cirrus above the contrail to zero. The reflected solar radiation at TOA is not available as a parameter in ERA-Interim, so it is taken from the short forecasts from the ECMWF IFS where (like the OLR) it is available as an accumulated value over the length of the forecast (6 or 12 hours). Instead of using accumulated forecast values of SDR, the accuracy of our calculations is improved by calculating the SDR hourly for each contrail point using the relation:

$$SDR = S_0 cos\theta \quad \text{(S4)}$$

where $cos\theta$ is the cosine of the solar zenith angle (calculated using the trajectory location, date and time) and S_0 is the solar constant adjusted to take account of the Earth's orbit. Note that in the hourly calculation of the SDR we increment only the time and not the location of the trajectory (i.e., we assume that the movement of the contrail is small enough not to affect these calculations). This is a reasonable approximation given that the majority (92%) of contrails in our dataset have a lifetime of less than six hours. Using these parameters, the SW RF is calculated hourly using Eqs. (5)-(10) in Schumann et al. (2012).

The area covered by each contrail is assumed constant along the contrail trajectory. Taking values from Grewe et al. (2014a), we use a contrail width W = 200 m, and a contrail length of the square root of the grid box area (we use a 1 degree by 1 degree grid). Grewe et al. (2014a) multiply the contrail length by the potential contrail coverage; this describes what fraction of the grid box may be covered by contrails (i.e., it would be reduced if the natural cirrus coverage is large). We do not attempt to calculate the potential contrail coverage (since it is calculated online in the climate model used in Grewe et al. (2014a)) and assume it is equal to 1.0 here.

The net RF was calculated at each point along the contrail trajectory. The calculation of total net RF for each contrail follows Grewe et al. (2014a); the net RF is converted to a global-mean value and integrated in time:

$$RF = \frac{1}{T}\int_{t_0}^{t_0+T} F(t)dt \quad \text{(S5)}$$

Where T = 1 yr.

S2. Derivation of Algorithmic Climate Cost Functions

Simple statistical methods were used to derive the algorithmic climate cost functions (aCCFs). The aCCFs were required to be derived in terms of the average temperature response climate metric with a 20-year time-horizon (ATR20), to be consistent with the aCCFs being derived by TU Delft and DLR for other aviation emissions. Since our contrail lifetime is fixed at 6 hours the conversion between the radiative forcing and ATR20 is a simple scaling by a factor of 0.0151 (calculated by Katrin Dahlmann at DLR). Hence we have derived the algorithmic climate cost functions in terms of RF; to convert to ATR20, they are multiplied by a factor of 0.0151.

The method used to calculate the contrail aCCF was based on van Manen and Grewe (2019) to derive the aCCF for water vapour, ozone, and methane. First, scatterplots of relevant meteorological variables against net RF were plotted to determine which parameters had the strongest relationships with net RF. Second, simple statistical methods were used to fit the data, starting with simple linear regression, progressing to a more complicated non-linear regression for the night-time contrail data. Each method was assessed by plotting the original net RF with the RF calculated using the aCCFs, and calculating the Spearman's rank correlation coefficient. In addition, for the daytime contrails we calculated the percentage of contrails for which the sign of the net RF was correctly calculated.

Results

A scatterplot of net RF versus contrail lifetime for all contrails in the new dataset is shown in Figure S2. 92% contrails have a lifetime of 6 hours or less; a few contrails have a lifetime of up to 48 hours. The majority of contrails have a net positive RF, which means they act to warm the climate. Some contrails have a net negative RF, so they would act to cool the climate; these only occur for contrails with lifetimes of up to 18 hours.

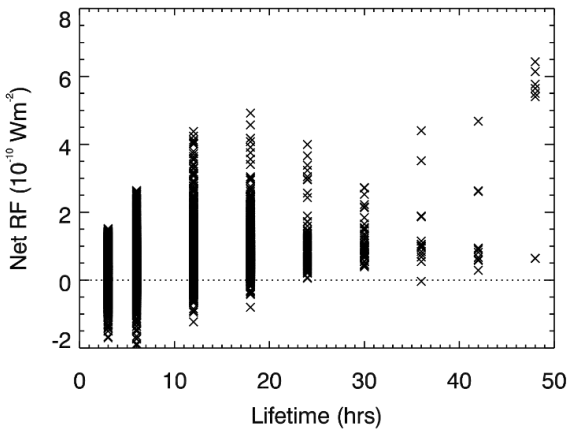

Figure S2: Scatterplot of net RF versus contrail lifetime, for all contrails in the new ATM4E contrail dataset

A constraint on deriving the algorithm is that only meteorological information available at the time of flight can be used. In addition, we restrict to conventional meteorological data, so that the algorithm is simple to implement. This means, for example, that we have no information on the contrail lifetime, since this is not something that can be estimated a priori from meteorological data. Since a lifetime is required to be input to the calculations of net RF, and in the conversion from RF to ATR20, we are forced to assume the same lifetime for all contrails. We have chosen to use a contrail lifetime of 6 hours, which seems a reasonable assumption given that 92% of contrails have lifetime of up to 6 hours.

Night-time and day-time contrails were analysed separately. Here, night-time contrails refer to contrails with their entire (6 hour) lifetime occurring at night. Since these contrails exist only during hours of darkness they have no shortwave forcing, only longwave forcing and hence their net RF must be positive (warming).

Day-time contrails are used to refer to contrails that form and dissipate during daylight or which have part of their lifetime during the day. The dependence of the net RF on the meteorological parameters is different for these two groups, since the net RF of night-time contrails has only a longwave RF component, which is largely dependent on temperature and outgoing longwave radiation. The net RF of day-time contrails is a balance between the net shortwave and net longwave components, so it includes a dependence on the solar zenith angle at the time of contrail formation.

Night-time contrails

The parametric equations to calculate the long-wave RF have a strong dependence on temperature and OLR. It is therefore unsurprising that the highest correlation of the RF with meteorological variables is with temperature (R=0.73), followed by OLR (R=0.63).

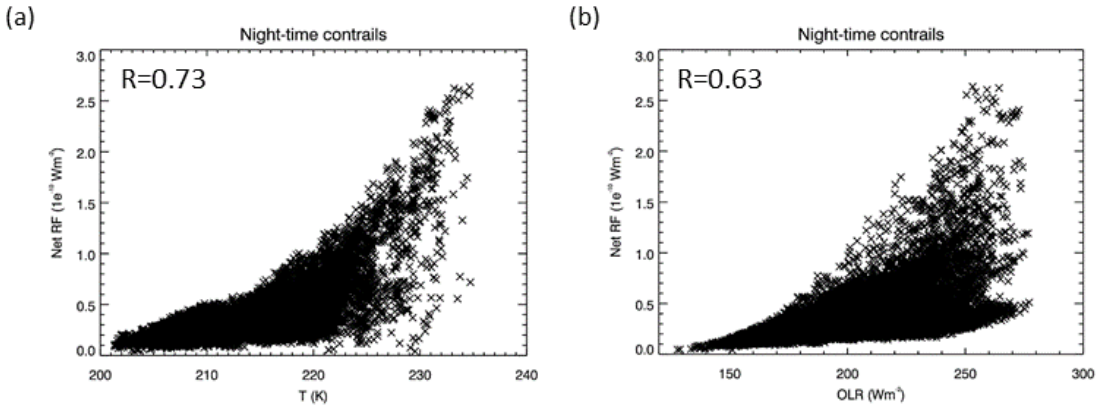

Figure S3: For night-time contrails with a lifetime of 6 hours, scatterplots of net RF versus (a) T and (b) OLR. Spearman's rank correlation coefficients (R values) are shown.

We initially tried to derive the aCCF using linear regression onto temperature since the temperature has the largest correlation with RF. Using a linear regression of net RF onto temperature results in Eq. (S6):

$$RF = 3.52e^{-12}T - 7.13e^{-10} \quad \text{(S6)}$$

However, using Eq. (S6) to estimate the net RF using only temperature results in a small number of negative RF values, when the net RF for night-time contrails can only be positive. Adding a second term to this formula by calculating a linear fit to the residuals against OLR does not improve the fit and increases the number of contrails for which the sign of net RF is predicted to be negative.

To ensure that the aCCF produces only positive values of net RF for night-time contrails, non-linear statistical fits were investigated. The fit shown here takes the form RF = a 10^(bT) + c, following the formulation of the equation for ice water content (Eq. (S1)). The motivation for this choice is that this expression is one of the main ways that temperature enters the calculation of RF in the parametric equations. Using statistical fitting, this results in Eq. (S7):

$$RF = 1e\text{-}10*(0.0073x10^{\,0.0107\,T} - 1.03) \quad \text{(S7)}$$

The nonlinear fit from Eq. (S7) is considered an improvement over Eq. (S6) since the fitted RF correctly predicts only positive RF values. Note that for this to be the case, Eq. (S7) is not valid for temperatures less than 201 K. In this instance, the RF should be set to 0 W m^{-2}; temperatures this low should be very rare (or non-existent) for

the range of altitudes and latitudes considered in ATM4E. In common with Eq. (S6), using Eq. (S7) results in an underestimation of the larger net RF values (see Figure S4 (b)).

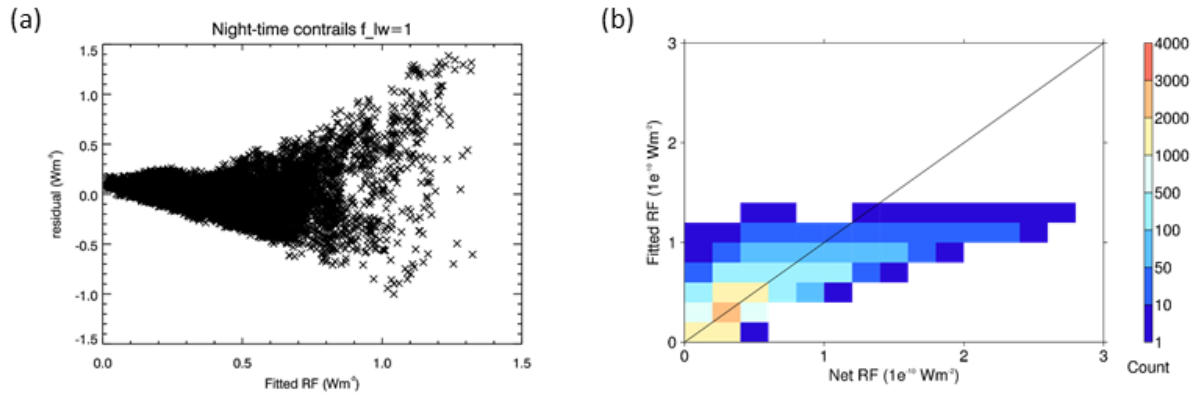

Figure S4: For night-time contrails with a 6-hour lifetime (a) scatterplot of the residual against the fitted RF (RF estimated using the aCCF). (b) density plot for the fitted RF versus net RF where the colour of the box represents the number of contrails.

The performance of the algorithm has also been assessed against the rest of the contrails in the dataset, which have a range of lifetimes between 3 hours and 48 hours. The fit is best for contrails with short lifetimes (Figure S5). The algorithm generally overestimates the net RF of contrails with a 3-hour lifetime (i.e., a shorter lifetime than the 6 hours used to derive the algorithm) and underestimates the net RF of contrails with lifetimes of 12 hours and above (i.e., longer lifetimes than the 6 hours used to derive the algorithm).

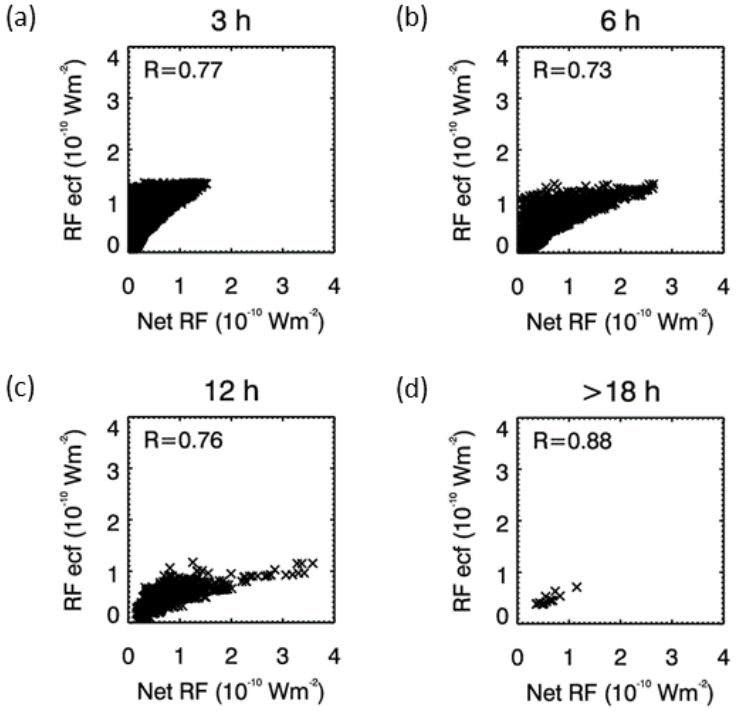

Figure S5: Scatterplots of the fitted RF (RF estimated using the aCCF) versus the net RF for night-time contrails with lifetime (a) 3, (b) 6, (c) 12 and (d) at least 18 hours. If the net RF and fitted RF were in perfect agreement the points would lie along the red line. Spearman's rank correlation coefficients (R values) are shown.

Day-time contrails

Here, day-time contrails refer to contrails which either form and dissipate during daylight hours or exist during both day-time and night-time. This means that the net RF for these contrails is a balance between the shortwave and longwave components and can be either positive (warming) or negative (cooling). This more complex situation leads to different relationships between net RF and meteorological variables than night-time contrails. The highest correlations between the net RF is now with OLR (R=0.86) and SZA (R=-0.47), and the net RF is

poorly correlated with temperature (R=0.08) (Figure S6). The correlation with solar zenith angle at the time of contrail formation would be lower if the dataset included contrails which formed at night and persisted into day-time (rather than only contrails forming in day-time). The correlation with OLR is not so straightforward to explain; OLR is used in the calculation of the LW RF, and would be influenced by natural cloud cover.

Initially, the aCCF were derived separately for contrails that existed only during daylight hours and those that existed during day and night. Since the dependence on meteorological variables and aCCF (not shown) were not significantly different, the data were combined into one dataset. This also has the advantage of increasing the size of the data sample (to over 10 000 contrails), making the statistical fits more robust.

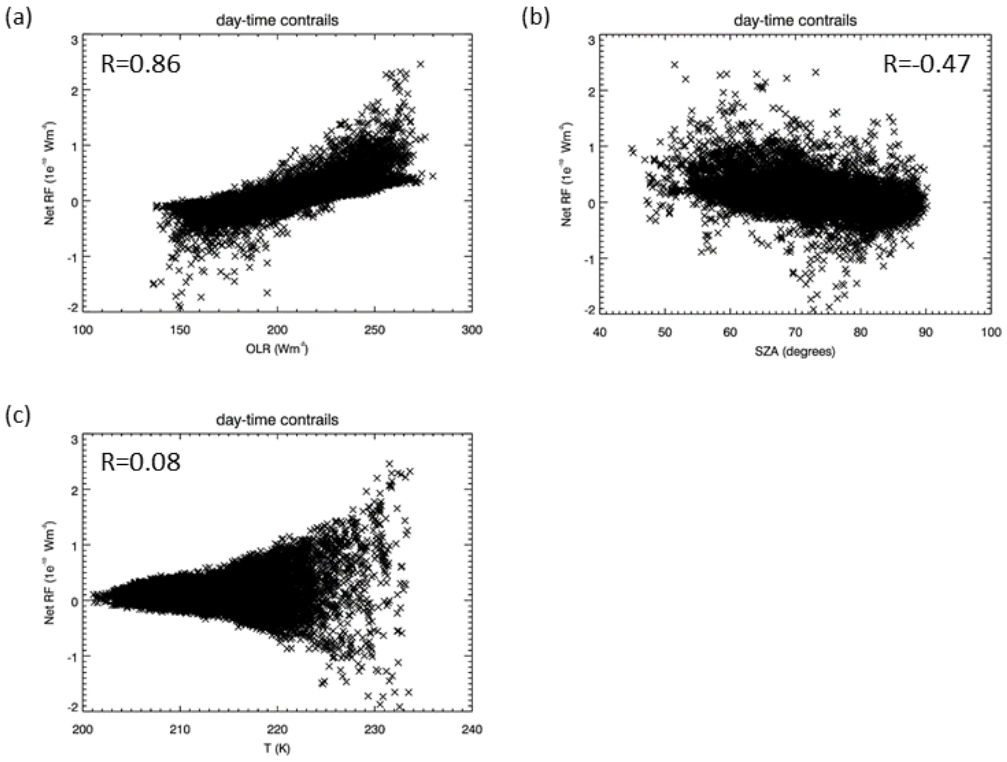

Figure S6: For day-time contrails scatterplots of net RF versus (a) OLR, (b) SZA and (c) T. Spearman's rank correlation coefficients (R values) are shown.

The aCCFs for day-time contrails are derived using linear regression of net RF onto OLR, since OLR has a high linear correlation with net RF. This results in the following aCCFs Eq. (S8):

$$RF=1e\text{-}10*(-1.7\text{-}0.0088*OLR) \quad (S8)$$

This produces a good fit between the net RF and fitted RF for contrails with a lifetime of 6 hours (Figure S7(a)). Importantly, the percentage of contrails for which the sign of RF is correctly predicted is high at 88%. The contrails whose RF is incorrectly predicted have small RF (Figure S7(b)); the sign of RF for contrails with larger net RF are correctly predicted. Note that Eq. (S8) will predict negative RF for OLR < -193 W m^{-2} and positive for larger values. The introduction of a second parameter (SZA or T) does not improve the fit. Moreover, SZA at the time of contrail formation cannot be used for contrails that form at night and persist into day-time.

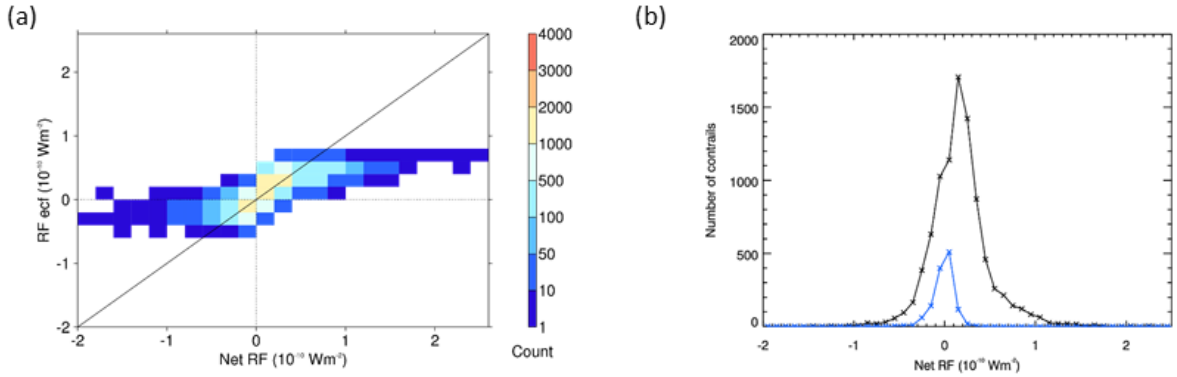

Figure S7: For day-time contrail data with a 6-hour lifetime (a) density plot for the fitted RF versus net RF where the colour of the box represents the number of contrails. (b) PDFs of net RF for contrails where the aCCFs correctly (black line) or incorrectly (blue line) predicts the sign of the forcing.

The performance of the algorithm was also assessed against the rest of the contrails in the dataset, which have a range of lifetimes between 3 hours and 48 hours. As for the night-time aCCFs the fit is best for contrails with short lifetimes of up to 6 hours (Figure S8). The fit and ability to correctly predict the sign of the forcing is similar for contrails with lifetimes of 3 and 6 hours. For contrails with lifetimes of 18 hours and longer, the larger values of net RF are underestimated, and the percentage of contrails where the sign of the RF is correctly predicted reduces to 77% (Figure S8 (d)). However, as for the 6-hour lifetime contrails, the contrails with the largest net RF have the sign of forcing correctly predicted, which provides confidence that using the algorithm will result in the correct routing decision.

Note that the night-time aCCF has an implicit dependence on contrail altitude since it depends on the temperature at the time of contrail formation. In this formulation, contrails formed at warmer temperatures (lower altitudes) have a higher forcing than those at higher altitudes and colder temperatures. The day-time aCCFs have no such dependence; the aCCFs calculated at any given location will be the same regardless of the altitude the contrail is formed at. The altitude dependence of the day-time contrail forcing could be investigated further (with a different dataset). We have also not investigated how the net RF depends on what fraction of the contrail lifetime is during day-time, since our contrails were initialised only at 2 different times of the day.

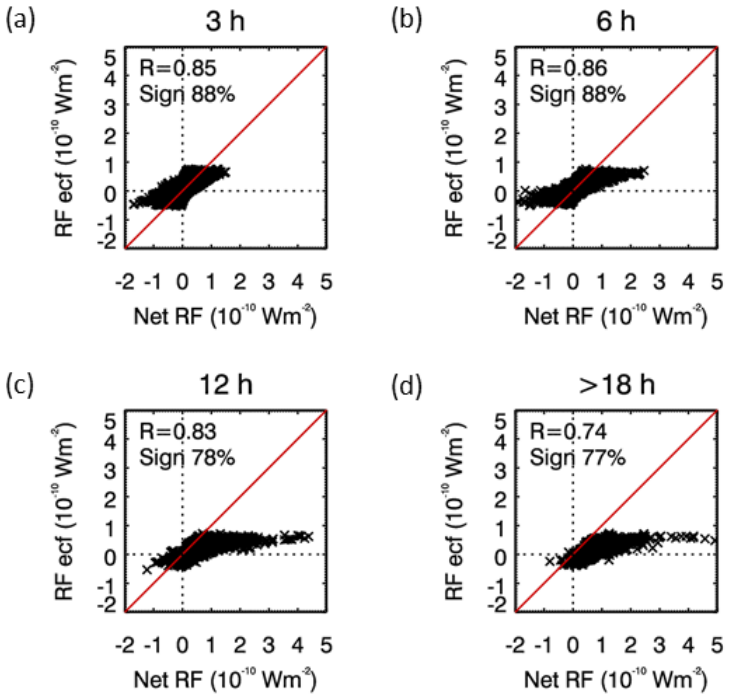

Figure S8: Scatterplots of the fitted RF (RF estimated using the aCCF) versus the net RF for day-time contrails with lifetime (a) 3, (b) 6, (c) 12 and (d) at least 18 hours. If the net RF and fitted RF were in perfect agreement the points would lie along the red line. Spearman's rank correlation coefficients (R values) and the percentage of contrails for which the sign of the aCCF RF is correct are shown.

References

Grewe, V., Frömming, C., Matthes, S., Brinkop, S., Ponater, M., Dietmüller, S., Jöckel, P., Garny, H., Tsati, E. and Dahlmann, K. (2014a). "Aircraft routing with minimal climate impact: the REACT4C climate cost function modelling approach (V1. 0)." Geoscientific Model Development, 7(1): 175-201.

Irvine, E. A., Hoskins, B. J. and Shine, K. P. (2014). "A Lagrangian analysis of ice-supersaturated air over the North Atlantic." Journal of Geophysical Research: Atmospheres, 119(1): 90-100. DOI: https://doi.org/10.1002/2013JD020251.

Methven, J. (1997). Offline trajectories: Calculation and accuracy. Department of Meteorology University of Reading.

Schumann, U., Baumann, R., Baumgardner, D., Bedka, S. T., Duda, D. P., Freudenthaler, V., Gayet, J. F., Heymsfield, A. J., Minnis, P., Quante, M., Raschke, E., Schlager, H., Vázquez-Navarro, M., Voigt, C. and Wang, Z. (2017). "Properties of individual contrails: a compilation of observations and some comparisons." Atmos. Chem. Phys., 17(1): 403-438. DOI: 10.5194/acp-17-403-2017.

Schumann, U., Mayer, B., Gierens, K., Unterstrasser, S., Jessberger, P., Petzold, A., Voigt, C. and Gayet, J.-F. (2011). "Effective Radius of Ice Particles in Cirrus and Contrails." Journal of the Atmospheric Sciences, 68(2): 300-321. DOI: 10.1175/2010jas3562.1.

Schumann, U., Mayer, B., Graf, K. and Mannstein, H. (2012). "A Parametric Radiative Forcing Model for Contrail Cirrus." Journal of Applied Meteorology and Climatology, 51(7): 1391-1406. DOI: 10.1175/jamc-d-11-0242.1.

Unterstrasser, S. and Gierens, K. (2010). "Numerical simulations of contrail-to-cirrus transition – Part 1: An extensive parametric study." Atmos. Chem. Phys., 10(4): 2017-2036. DOI: 10.5194/acp-10-2017-2010.

van Manen, J. and Grewe, V. (2019). "Algorithmic climate change functions for the use in eco-efficient flight planning." Transportation Research Part D: Transport and Environment, 67: 388-405. DOI: https://doi.org/10.1016/j.trd.2018.12.016.